Turning off Hydrogen To Realize Seeded Growth of Subcentimeter Single-Crystal Graphene Grains on Copper

Lin Gan and Zhengtang Luo*

Department of Chemical and Biomolecular Engineering, The Hong Kong University of Science and Technology, Clear Water Bay, Kowloon, Hong Kong

ABSTRACT Subcentimeter single-crystalline graphene grains, with diameter up to 5.9 mm, have been successfully synthesized by tuning the nucleation density during atmospheric pressure chemical vapor deposition. Morphology studies show the existence of a single large nanoparticle (>∼20 nm in diameter) at the geometric center of those graphene grains. Similar size particles were produced by slightly oxidizing the copper surface to obtain oxide nanoparticles in Ar-only environments, followed by reduction into large copper nanoparticles under H_2/Ar environment, and are thus explained to be the main constituent nuclei for graphene growth. On this basis, we were able to control the nanoparticle density by adjusting the degree of oxidation and hydrogen annealing duration, thereby controlling nucleation density and consequently controlling graphene grain sizes. In addition, we found that hydrogen plays dual roles on copper morphology during the whole growth process, that is, removing surface irregularities and, at the same time, etching the copper surface to produce small nanoparticles that have only limited effect on nucleation for graphene growth. Our reported approach provides a highly efficient method for production of graphene film with long-range electronic connectivity and structure coherence.

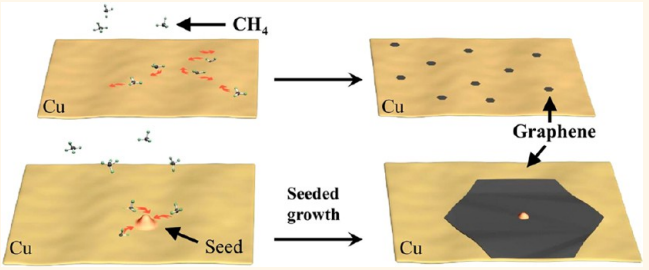

KEYWORDS: graphene · single-crystal graphene · seeded growth · chemical vapor deposition · grain boundary

Grain sizes are crucial parameters dominating the properties of polycrystalline materials. This is especially critical for two-dimensional materials including graphene thin film, where grain boundaries will disrupt electronic connectivity and structural continuity, resulting in low charge carrier mobility[1−3] and poor mechanical properties.[4,5] On the other hand, it is desirable to have single-crystal graphene flakes with dimensions comparable to microprocessors, henceforth to completely avoid electrical uncertainties at the grain boundaries. To increase the graphene sizes and to reduce the defect density, eventually to improve the ultimate properties of graphene structures, our previous work has shown that surface morphology of the Cu substrate and feedstock precursor concentration are the dominant factors controlling defect density and grain size.[6−8] For this, the previous main strategy is to flatten the catalytic copper surface, thus reducing surface irregularities, which otherwise will function as a random active site and form abundant nucleation center, and limits the graphene grain size, along with increasing fraction of the grain boundaries.[9−11] More recently, many other methods have also been developed for this goal, such as electropolishing,[7] elongated substrate annealing time (up to 7 h),[12] switching to melted substrate,[9] separating into an low and high feedstock growth,[2] and annealing at high pressure followed by low-pressure growth.[12] With these methods, along with optimized growth conditions such as optimal H_2/CH_4 ratio, graphene flakes with millimeter diameters were reported.[12,13] Unfortunately, only limited success for the growth of centimeter size graphene flakes was achieved by using the above-mentioned conventional strategies.[12] Another promising strategy is to introduce a higher selective catalyst during graphene nucleation, which reduces the nucleation density,[11] and henceforth limits the total number of graphene grains in the growth stage, allowing nuclei to grow into large grains before they merge.

* Address correspondence to keztluo@ust.hk.

Received for review August 22, 2013 and accepted September 23, 2013.

Published online September 23, 2013
10.1021/nn404393b

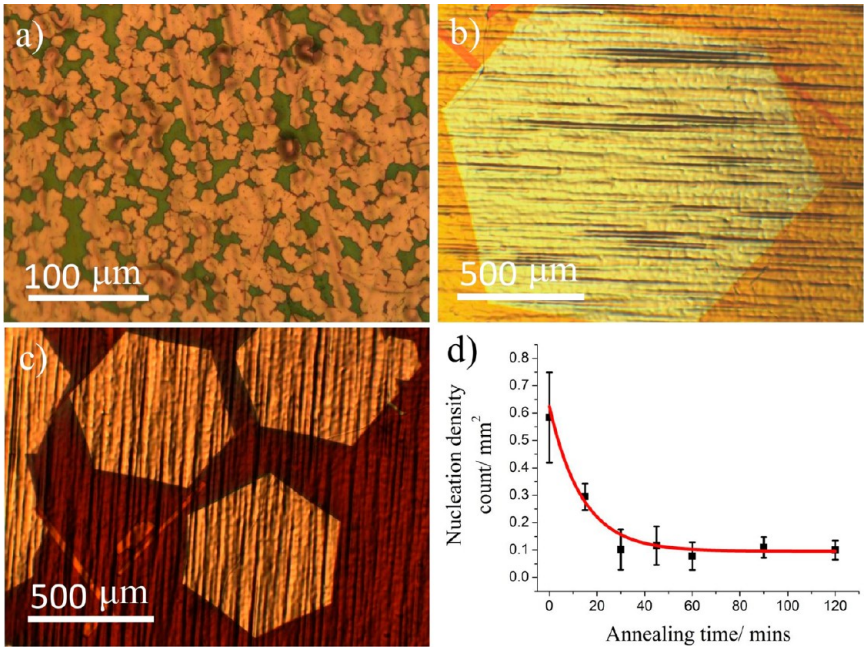

Figure 1. Optical images of graphene grains grown on copper foil of various preheating conditions: (a) preheated in Ar/H_2 mixture; (b) preheated in Ar only; (c) preheated in air at 200 °C for 5 min. (d) Plot and fit of graphene flake density curve as a function of annealing time. For (d), copper foil was preheated in Ar only but annealed in Ar/H_2.

Here, we demonstrate that the critical issue of controlling the nucleation density is solved by "seeding" the catalytic metal surface with nucleation sites for graphene growth, which then defines the number of graphene grains in the graphene growth process and allows us to grow grains to large sizes. By seeding the chemical vapor deposition of methane, we achieve a high yield of hexagonal single-crystal grains of graphene, whose dimension grows to an order of magnitude larger than conventional CVD graphene grains. Our technique eliminates the needs to obtain a flat catalytic surface using complicated surface treatments such as tenuous polishing or elongated annealing.

The single-layer graphene growth method used here is based on the established atmospheric pressure chemical vapor deposition methods using Cu foil as catalyst (see Supporting Information for more details).[3,7] Copper foil is mechanically polished (10−15 s supersonic treatment) on both sides with etchant solution (5 g of $FeCl_3$, 10 mL of HCl, and 100 mL of DI water) and then rinsed with DI water three times, followed by nitrogen blow-dry before growth. The key modification in this current method is that, during the preheating step (*i.e.*, increase temperature from room temperature to growth temperature at 1050 °C), only argon gas (320 sccm, Hong Kong Specialty Gases Co., Ltd., 99.999%, oxygen concentration <3 ppm) is used, as opposed to the Ar/H_2 mixtures used by conventional CVD graphene growth processes. As will be discussed in detail later in the text, this step is crucial in introducing the nucleation centers in the graphene growth step and consequently enables us to control the graphene size. This step is followed by hydrogen annealing (Hong Kong Specialty Gases Co., Ltd., 99.999%, oxygen concentration <5 ppm) for a chosen period. After that, 15 sccm of methane/Ar (500 ppm methane diluted in argon, Arkonic Gases and Chemicals Inc., 99.99%) is charged into the system to start the graphene growth. After this growth step, the furnace is turned off and slides away to fast-cool the copper/graphene sample. Finally, methane and hydrogen flow is switched off when the system is cooled to room temperature. In summary, we used three steps in the graphene growth process: (1) preheating step, that is, to raise the temperature from room temperature to growth temperature; (2) annealing in Ar/H_2 at the growth temperature; and (3) deposition of graphene.

RESULTS AND DISCUSSION

Crucially, with the presence of hydrogen during the preheating step, the overwhelming majority of graphene grains are only a few dozens of micrometers in diameter, shown in Figure 1a, similar to results obtained by other researchers.[3] Figure 1a,b illustrates graphene grains obtained from a growth process with preheating in Ar/H_2 and Ar only, respectively. Here we use the reported graphene visualization methods,[14,15] where the graphene/copper sample is oxidized in air and results in a reflective contrast between the oxidized copper in the exposed regions and the unexposed copper covered by graphene. This simple technique allows us to immediately obtain size and morphology information of the graphene flakes on the copper foil. Assuming that each resulting graphene hexagonal flake formed from a single nucleation center,[3] one can observe a ~17 000-fold reduction

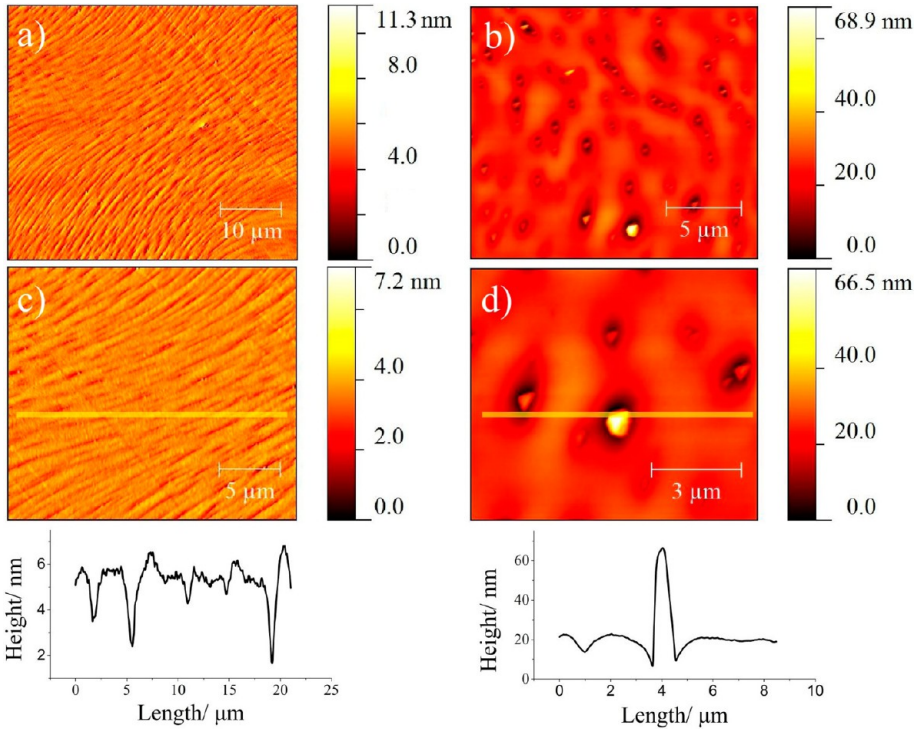

Figure 2. AFM images of copper foil with Ar-only and Ar/H_2 preheating. (a,c) Preheated in Ar/H_2 mixture, (b,d) preheated in Ar only. Preheating in Ar/H_2 mixture resulted in a rather low roughness surface, while heating in Ar obtains a surface decorated with a high density of nanoparticles.

of nucleation density, corresponding ~10 000 and ~0.6 nuclei/mm^2 in Figure 1a,b, respectively. Here the nucleation density is calculated from the whole surface of the copper substrate with size of 2 × 4 cm^2 (see Figure S3 in the Supporting Information). In addition, graphene flakes in both images are a highly symmetric hexagonal shape, indicating the single-crystal nature of the graphene flakes, consistent with previous observations, and will be discussed in more detail later in the text.[3] Since the major function of hydrogen during the preheating step is to eliminate trace amount of oxygen that is from either the Ar carrier gas or residual oxygen in the system, one might expect that oxygen plays a vital role in this preheating process.

To determine the role of oxygen in the preheating process, we preheat the copper foil in air (*i.e.*, with higher concentration of oxygen) at 200 °C for 5 min as a control experiment, instead of preheating in Ar only or Ar/H_2, and then go through the same graphene growth process as the conventional method (*i.e.*, annealing in the Ar/H_2 environment and a normal growth). As expected, nucleation density of ~5 nuclei/mm^2 was obtained, a little higher but comparable to the Ar-only preheating process, shown in Figure 1c. This control experiment confirmed our hypothesis that oxygen plays a vital role in decreasing nucleation density, while on the contrary, preheating in Ar/H_2 resulted in high nucleation density. The significant decrease of nucleation density is also observed even the Ar/H_2 annealing step is omitted after preheating (data not shown).

Having clarified the important role of oxygen in the preheating step of significantly reducing nucleation density, we next investigated how to fine-tune the nucleation density during the Ar/H_2 annealing step. Figure 1d illustrates the graphene flake density (*i.e.*, nucleation density) as a function of Ar/H_2 annealing time during the annealing step, where an Ar-only atmosphere was used in the preheating step. In Figure 1d, we show how the number of graphene seeds and, consequently, the average size of graphene grains (inversely proportional to number of seeds) can be tuned an order of magnitude by varying the annealing time from 0 to 120 min in the Ar/H_2 annealing step. The nucleation density rapidly decreases for annealing time shorter than 30 min and levels off beyond this point. This finding is consistent with previous experimental observations that elongated hydrogen annealing assists the removal of surface irregularity, which in turn reduces the "active sites" and finally enables large graphene grains to be obtained.[12,16]

We further probed the effect of oxygen on nucleation density reduction by comparing the surface morphology after preheating in Ar/H_2 and Ar only environments using atomic force microscopy (AFM). Figure 2a,c and 2b,d compare the AFM images of Cu foil that are preheated in Ar/H_2 and Ar only, respectively, both annealed in Ar/H_2 for 30 min, a step used by the conventional CVD graphene growth method and the method in this report. Here, preheating in an Ar/H_2 environment has a short-range smoothing effect, consistent with previous reports

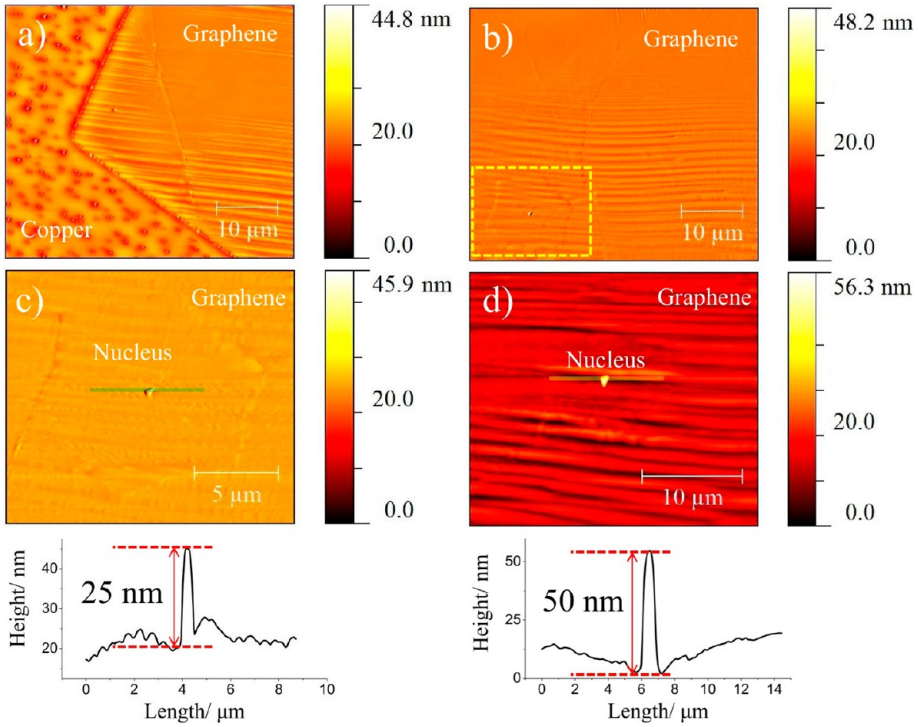

Figure 3. Postgrowth copper foil/graphene morphology. (a) Boundary region, showing sharp contrast of nanoparticle density between graphene-covered and exposed regions. (b) Graphene flake center region; a hexagonal shape nucleus with a nanoparticle is observed. (c,d) Typical AFM images of graphene nucleus with nanoparticles in the center.

that high temperature hydrogen annealing has a smoothing effect on copper.[16] However, the long-range morphology exhibits a fluctuating appearance with decorated pits (Figure S2c), consistent with recent observations.[17] In contrast, preheating in an Ar-only environment produces a rather rough and uniform surface (Figure S2d) with copper oxide nanoparticles, which were reduced to Cu nanoparticles after Ar/H_2 annealing,[18] with sizes of several to tens of nanometers randomly distributed on the whole surface of the copper foil. In fact, the formation of copper oxide nanoparticles/nanowires had been widely recorded, and it is proven that oxide nanowires/nanoparticles will be formed on the stressed region,[19] but only oxide particles with diameters on the micrometer scale will be formed at the temperature of >700 °C,[20] consistent with this observation if the difference of oxygen and heating time are considered between our systems.

Further insight into the role of nanoparticles can be gained by examining the postgrowth morphology of the Cu surface, as well as graphene structures produced after the growth. Figure 3a,b illustrates typical graphene/Cu boundaries and center of graphene flakes. Figure 3a demonstrates distinct features on the graphene-covered area and exposed Cu surfaces. Dense nanoparticles were observed in the exposed regions, consistent with previous reports.[20] In contrast, in the graphene-covered area, only the nanoparticles in the grain boundary and nucleus center (Figure 3b) are visible. Interestingly, we also observed dense graphene wrinkles that arose from postgrowth cooling due to differential thermal expansion of the metal substrate and graphene.[21,22] On the other hand, the center of the graphene flakes normally shows a few-layer structure with a nanoparticle in the geometrical center of the hexagons, as shown in Figure 3c,d. The size of the nanoparticles in the grain center normally are larger than 20 nm and show many similarities to the nanoparticles observed in Figure 2b,d, indicating to us that nanoparticles produced in the preheating then reduced in the annealing step are likely to be the nucleation center during the graphene growth step.

The fact that the density of the obtained graphene flake is significantly lower than the density of nanoparticles of >20 nm diameter indicates that only a small portion of the nanoparticle can form the nucleation center during the graphene growth. To investigate the evolution of nanoparticle size distribution, we studied the morphology of Cu foil that undergoes Ar-only preheating and Ar/H_2 annealing for 5, 40, and 90 min, as listed in Figure 4a−c, respectively, with corresponding nanoparticle size distributions shown in Figure 4d−f, as well as their pie chart of two size categories divided by 20 nm diameter. From the initial annealing, a certain density of large size nanoparticles already exists on the Cu surface, and more particles continued to appear as we increased the Ar/H_2 annealing time. Subsequently, the total number of nanoparticles increases significantly. However, a more detailed inspection into the nanoparticle size distributions (Figure 4d−f) reveals that the nanoparticle indeed shows a bimodal distribution, with a ~20−40 nm diameter gap.

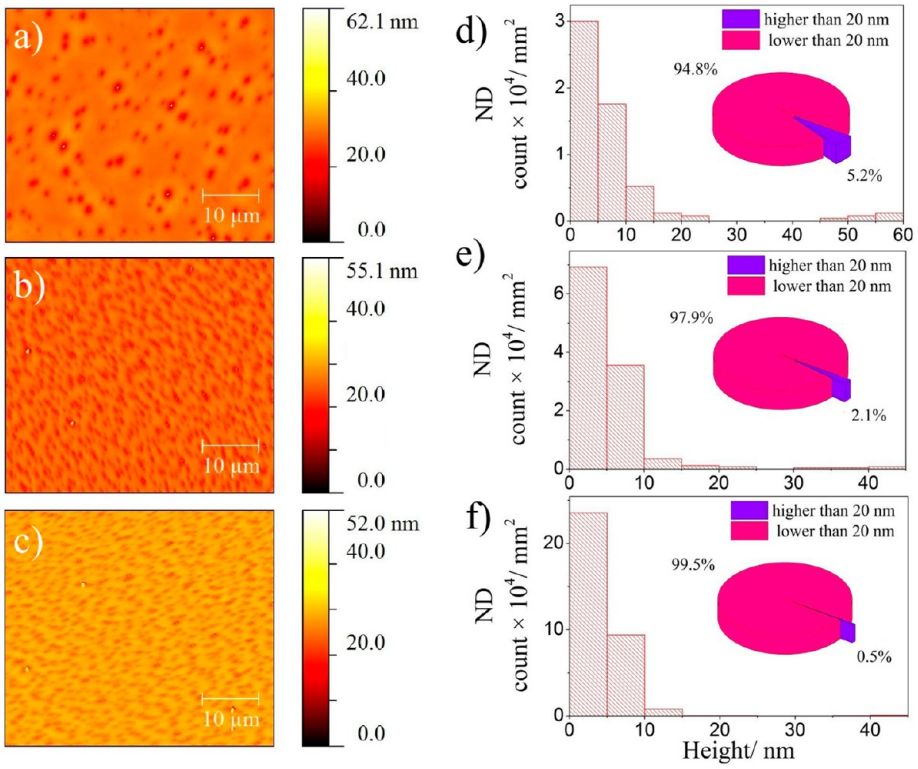

Figure 4. Cu foil morphology and histogram of nanoparticle sizes at various hydrogen annealing time: (a,d) 5 min annealing; (b,e) 40 min annealing; (c,f) 90 min annealing. Pie charts in the insets depict the fraction of nanoparticles with diameter higher/ lower than 20 nm.

Here, we choose 20 nm as a dividing line for convenience. A pie chart of the nanoparticle populations for these two nanoparticle categories (<20 and >20 nm, respectively) shows that the fraction of nanoparticles with >20 nm diameter is only a small portion of nanoparticles. More importantly, both the fraction and total numbers of them in all nanoparticles (Figure 5a) are really decreasing with increasing of annealing time, as opposed to the overall nanoparticle population increase.

Plot of density of nanoparticles with >20 nm diameter as an function of annealing duration is also presented in Figure 5a, along with variation of nucleation density, previously presented in Figure 1d. Here, these two curves show a very good match, signifying the link between the population of the >20 nm nanoparticles and the number of nuclei that lead to the growth of hexagonal graphene grains. In fact, for the nanoparticles that are in the center of hexagonal graphene flakes, 90% (18 out of 20) of the measured nanoparticles has a diameter larger than 20 nm, consistent with the hypothesis that only a certain set of nanoparticles produced in the preheating and annealing step becomes the nucleation center. At the current stage, it is not clear why the nucleation centers are normally associated with large nanoparticles. A closer inspection of the line profile from the AFM images, such as those in Figure 5b, reveals that small nanoparticles may have a greater chance to be trapped in the valley of the Cu surface and thus reduce their exposure to dilute methane, while larger nanoparticles have more chance to catalyze the crack of methane during the CVD process, as they have more exposure to the environment. Further studies are underway to elucidate this size effect. In short, although the whole numbers of nanoparticles are increasing with extended annealing time, the amount of large nanoparticles (>20 nm) that plays a vital role in nucleation is really decreasing at the same time, which suggests that the large nanoparticles (>20 nm) are introduced by oxidation during preheating rather than the Ar/H_2 annealing process; this point is also supported by Xia's work.[20] At the current stage, it is unclear why nucleation is mostly observed on nanoparticles with diameters >20 nm, while copper edges,[23] boundaries,[10] or even graphene edges[24] have also been reported as a nucleation site. A potential explanation is that the methane under extremely low concentrations in our experiments may have fewer chances to nucleate the aforementioned small irregularities before they nucleate those >20 nm nanoparticles.

On the basis of the above discussion, we conclude that hydrogen also has dual roles in reconstructing the Cu surface: (1) to smooth the Cu surface and remove the irregularities which otherwise may become the active center and initiate graphene growth, a convention method used to grow large graphene flakes; and (2) to etch the Cu surface and form new nanoparticles. This is similar to the dual role of

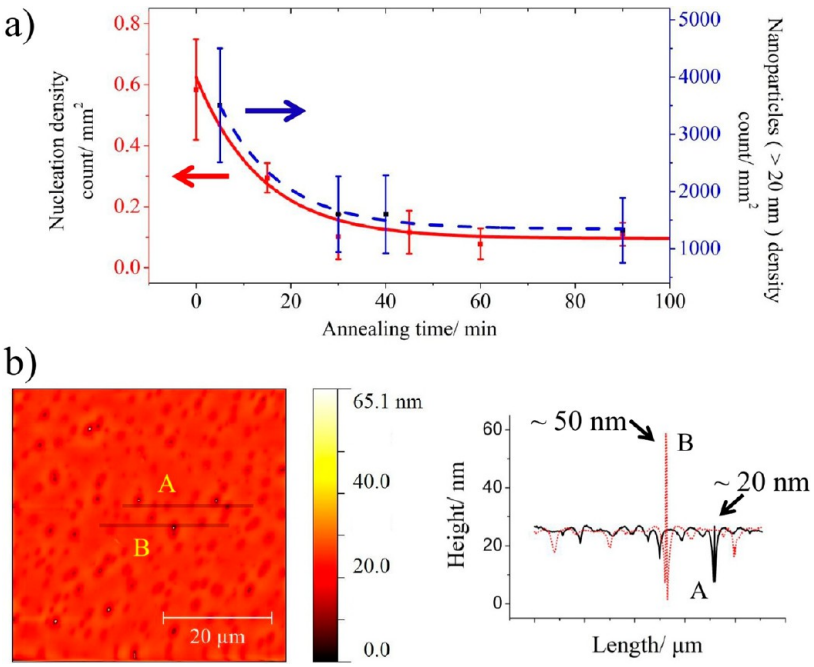

Figure 5. Correlation of nanoparticles of >20 nm in diameter and nucleation center nanoparticles. (a) Plot and fit of nucleation density (left *y*-axis) and population of nanoparticles with diameters larger than 20 nm (right *y*-axis) as a function of annealing time. The two curves show similar trends. (b) Typical profiles of nanoparticles with different height. The nanoparticles with a diameter >20 nm have more exposure to the carbon source during growth.

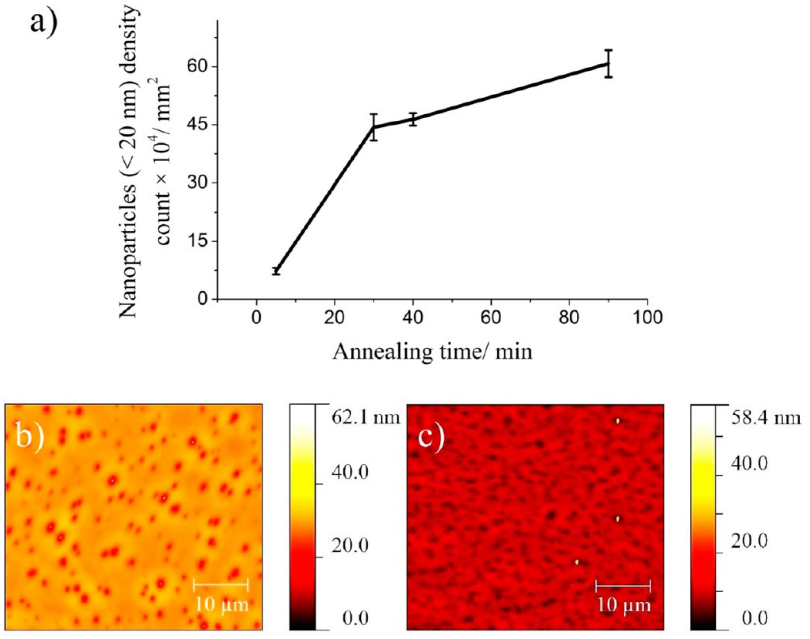

Figure 6. Nanoparticles generated by hydrogen annealing on the copper surface. (a) Density of nanoparticles with a diameter smaller than 20 nm as a function of annealing time in 6.2% hydrogen in Ar. The copper foils are annealed in Ar/H_2 for 5 min at hydrogen concentrations of (b) 6.2% and (c) 13.5%.

hydrogen in graphene growth: an activator of the surface-bound carbon and an etching reagent that controls the size and morphology of the graphene domains.[25] Figure 6a illustrates the density of small sized nanoparticles (<20 nm) as a function of Ar/H_2 annealing, extracted from Figure 4a–c. Unlike >20 nm nanoparticles produced by oxidation, these <20 nm small nanoparticles apparently result from hydrogen etching, as demonstrated by results from the following control experiments. Figure 6b,c demonstrates the AFM morphology of the Cu surface annealed for 5 min in Ar/H_2 gas with 6.2 and 13.5% hydrogen concentration, respectively. The nanoparticle density obtained by 13.5% hydrogen annealing (Figure 6b) is

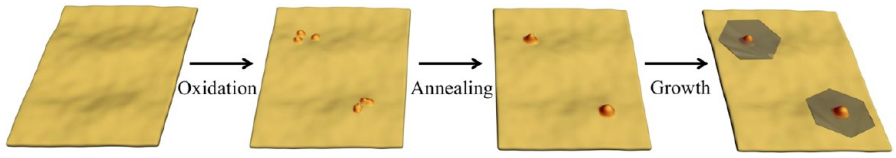

Figure 7. Scheme depicting the proposed mechanism for graphene seeded growth. (1) Formation of large nanoparticles resulting from the mild oxidation by trace amounts of oxygen in Ar gas or the CVD chamber. (2) Ar/H_2 annealing induces hydrogen etching and coalescence of nanoparticles. (3) Nucleation on the large nanoparticles (mainly on particles with diameter larger than 20 nm) and growth of graphene hexagon flakes.

higher than that those annealed in 6.2% hydrogen (Figure 6c). These results point to the hydrogen etching as the driving force for small nanoparticle production. Evidence of nanoparticles produced by hydrogen etching can be also found in Figure 2a,c, where a small fraction of nanoparticles can also be found.

Based on above findings, the following three-stage mechanism was proposed for the growth of large size graphene grain, shown in Figure 7. (1) Formation of large sized nanoparticles (>20 nm) results from the mild oxidation by a trace amount of oxygen in Ar gas or the CVD chamber. (2) Ar/H_2 annealing induces a decrease of existing large sized nanoparticles (>20 nm) and also introduces new small sized nanoparticles (<20 nm) by etching effect on copper. (3) Nucleation occurs on the large nanoparticles (mainly on particles with diameter larger than 20 nm) and growth of graphene hexagon flakes. In this mechanism, large sized nanoparticles (>20 nm) are to be the catalyst with nucleation probability higher than that of small sized nanoparticles (<20 nm) or the bulk copper surface, supported by our experiment results.

By using Ar-only annealing in the preheating step, followed by annealing for 30 min in Ar/H_2, we are able to significantly reduce the nucleation density and obtain graphene sizes of 5.9 mm in diameter, shown in Figure 8a, where a few hexagonal grains merge together. Our results indicate that, with sufficient low nucleation density, very large graphene flakes with a highly symmetric hexagonal shape can be obtained. Using such large grains, organic thin film transistors, and potentially large organic electronic circuits can be entirely fabricated on a single grain, thus completely avoiding the detrimental effects from the boundaries. Figure 8b shows the histogram of graphene grain size distribution of this sample.

Proof of the single-crystal nature of the graphene flakes grown from this method comes from the structure information by Raman measurement and selected area electron diffraction (SAED) spectrum by transmission electron microscopy (TEM) observation, shown in Figure 9a,b, respectively. As can be seen in Figure 9a, the intensity of the 2D peak (2696 cm^{-1}) shows only one Lorentz component and has an intensity 4 times higher than that of the G peak (1585 cm^{-1}), similar to pristine exfoliated graphene flakes from HOPG.[26] This

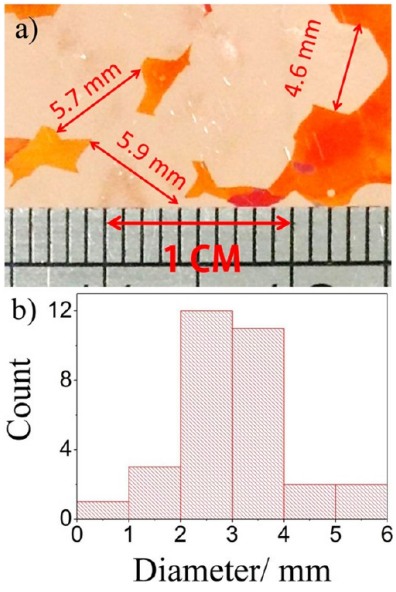

Figure 8. Merged subcentimeter single-crystal graphene grains grown on copper and their diameter distribution. (a) Optical image on oxidized Cu foil; (b) histogram.

supports our above-mentioned observation of the single-layer nature of those graphene flakes grown by this method. On the other hand, the weak intensity of the D peak (1354 cm^{-1}) confirms that our graphene structures have insignificant amounts of defects, consistent with previous work. To confirm this, we also obtain the lattice structures in 13 random locations (at least 40 μm apart) on the graphene and 800 μm graphene flakes, as shown in Figure 9b, using their SAED pattern. The SAED images are very sharp and show high crystalline nature, consistent with the above optical images and Raman measurement. Moreover, those 13 six-folded symmetrical SAED patterns exactly coincide with each other, providing direct evidence for the same hexagon lattice structure on the graphene flake.[12] The structure uniformity on the graphene flakes can be obtained by mapping the graphene flakes with Raman spectroscopy, shown in Figure 9c. As shown, the intensities of the 2D, G, and D peaks of graphene are homogeneous and continuous, indicating good structure uniformity, consistent with the SAED measurements. The ratio of I_D/I_G maintains a value in the range of 0–0.05, reflecting very low defects on those flakes.

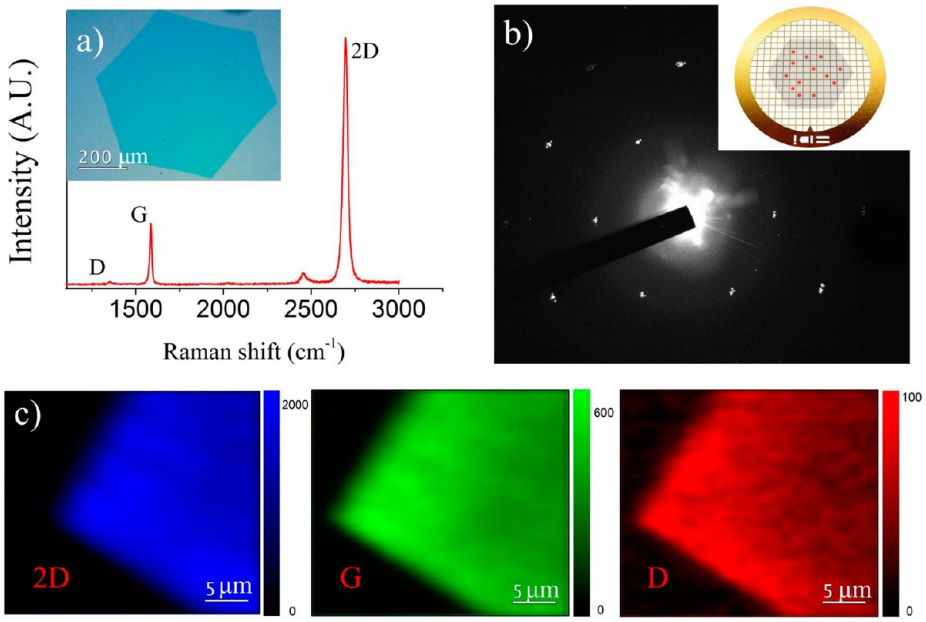

Figure 9. Characterizations of large sized single-crystal grains. (a) Raman spectrum of graphene transferred on silicon wafer, shown in the inset. (b) Electronic diffraction pattern formed by 13 separated SAED images; inset depicts the 13 randomly selected sites. (c) Raman intensity mapping results of 2D, G, and D bands on a corner of a hexagonal graphene flake.

CONCLUSION

In conclusion, we demonstrate a novel, highly effective method for synthesizing subcentimeter (up to 5.9 mm in diameter) single-crystal graphene grains based on seeding nanoparticles on the Cu surface. Those seeds can be introduced by preheating in Ar-only environments, followed by annealing in Ar/H_2 gas mixtures to fine-tune the density of the nanoparticles. AFM investigation on the prepared graphene flakes shows that a single nanoparticle with a diameter of $>\sim$20 nm was found in the center of graphene grains, indicating that only certain size nanoparticles (>20 nm in our experiment condition) can become the nucleation center during the graphene growth process. Plot of nucleation density at various annealing time matches well with the trend of the population of nanoparticles with diameters >20 nm, supporting strong correspondence between the nucleation particles and the large nanoparticles. On the basis of the above findings, we proposed the following stages during this seeded growth of graphene flakes: (1) large particle formation by the mild oxidation. (2) Ar/H_2 annealing induces a decrease in the number of existing large sized nanoparticles (>20 nm) and also introduces new small sized nanoparticles (<20 nm) by etching effect on copper. (3) Nucleation on the large nanoparticles and growth of graphene hexagon flakes. In addition, we demonstrate that hydrogen also has dual effects on the copper surface: smoothing and etching. Here we demonstrate that this method works well for large size graphene growth, but this method also is believed to have great potential for application in other 2D material synthesis.

During the revision of this article, we noticed the publication of an independent but similar work.[27] We believe that the current article provides, for the first time, the role of hydrogen during the seeded growth process.

METHODS

A SAED pattern was obtained using a JEOL 2010F operated at 200 keV. SEM was performed using a JEOL 6390 scanning electron microscope operated at 20 keV. The Raman spectrum was recorded with a Renishaw Raman RM3000 scope using a 514 nm excitation argon laser. AFM was scanned under semicontact mode using a NTEGRA probe NanoLaboratory (NT-MDT, Inc.) with ACTA tips from AppNano at 1.5 Hz scan rate and 512 × 512 resolution. Optical images were taken by a LEICA DFC 290 optical microscope. XPS spectrum was done using an Axis Ultra DLD with Al Kα X-ray source.

Conflict of Interest: The authors declare no competing financial interest.

Acknowledgment. This project is supported by the Research Grant Council of Hong Kong SAR (Project Number 623512). Technical assistance from the Materials Characterization and Preparation Facilities is greatly appreciated.

Supporting Information Available: Further details are provided related to graphene growth procedures, graphene transfer method, and chemical polishing method. This material is available free of charge *via* the Internet at http://pubs.acs.org.

REFERENCES AND NOTES

1. Yazyev, O. V.; Louie, S. G. Electronic Transport in Polycrystalline Graphene. *Nat. Mater.* **2010**, *9*, 806–809.
2. Li, X. S.; Magnuson, C. W.; Venugopal, A.; An, J. H.; Suk, J. W.; Han, B. Y.; Borysiak, M.; Cai, W. W.; Velamakanni, A.; Zhu, Y. W.; *et al.* Graphene Films with Large Domain Size by a Two-Step Chemical Vapor Deposition Process. *Nano Lett.* **2010**, *10*, 4328–4334.

3. Yu, Q. K.; Jauregui, L. A.; Wu, W.; Colby, R.; Tian, J. F.; Su, Z. H.; Cao, H. L.; Liu, Z. H.; Pandey, D.; Wei, D. G.; *et al.* Control and Characterization of Individual Grains and Grain Boundaries in Graphene Grown by Chemical Vapour Deposition. *Nat. Mater.* **2011**, *10*, 443–449.
4. Huang, P. Y.; Ruiz-Vargas, C. S.; van der Zande, A. M.; Whitney, W. S.; Levendorf, M. P.; Kevek, J. W.; Garg, S.; Alden, J. S.; Hustedt, C. J.; Zhu, Y.; *et al.* Grains and Grain Boundaries in Single-Layer Graphene Atomic Patchwork Quilts. *Nature* **2011**, *469*, 389–392.
5. Ruiz-Vargas, C. S.; Zhuang, H. L.; Huang, P. Y.; van der Zande, A. M.; Garg, S.; McEuen, P. L.; Muller, D. A.; Hennig, R. G.; Park, J. Softened Elastic Response and Unzipping in Chemical Vapor Deposition Graphene Membranes. *Nano Lett.* **2011**, *11*, 2259–2263.
6. Luo, Z. T.; Kim, S.; Kawamoto, N.; Rappe, A. M.; Johnson, A. T. C. Growth Mechanism of Hexagonal-Shape Graphene Flakes with Zigzag Edges. *ACS Nano* **2011**, *5*, 9154–9160.
7. Luo, Z. T.; Lu, Y.; Singer, D. W.; Berck, M. E.; Somers, L. A.; Goldsmith, B. R.; Johnson, A. T. C. Effect of Substrate Roughness and Feedstock Concentration on Growth of Wafer-Scale Graphene at Atmospheric Pressure. *Chem. Mater.* **2011**, *23*, 1441–1447.
8. Luo, Z. T.; Pinto, N. J.; Davila, Y.; Johnson, A. T. C. Controlled Doping of Graphene Using Ultraviolet Irradiation. *Appl. Phys. Lett.* **2012**, *100*, 253108.
9. Wu, Y. M. A.; Fan, Y.; Speller, S.; Creeth, G. L.; Sadowski, J. T.; He, K.; Robertson, A. W.; Allen, C. S.; Warner, J. H. Large Single Crystals of Graphene on Melted Copper Using Chemical Vapor Deposition. *ACS Nano* **2012**, *6*, 5010–5017.
10. Han, G. H.; Gunes, F.; Bae, J. J.; Kim, E. S.; Chae, S. J.; Shin, H. J.; Choi, J. Y.; Pribat, D.; Lee, Y. H. Influence of Copper Morphology in Forming Nucleation Seeds for Graphene Growth. *Nano Lett.* **2011**, *11*, 4144–4148.
11. Ajayan, P. M.; Yakobson, B. I. Graphene Pushing the Boundaries. *Nat. Mater.* **2011**, *10*, 415–417.
12. Yan, Z.; Lin, J.; Peng, Z. W.; Sun, Z. Z.; Zhu, Y.; Li, L.; Xiang, C. S.; Samuel, E. L.; Kittrell, C.; Tour, J. M. Toward the Synthesis of Wafer-Scale Single-Crystal Graphene on Copper Foils. *ACS Nano* **2012**, *6*, 9110–9117.
13. Gao, L.; Ren, W.; Xu, H.; Jin, L.; Wang, Z.; Ma, T.; Ma, L.-P.; Zhang, Z.; Fu, Q.; Peng, L.-M.; *et al.* Repeated Growth and Bubbling Transfer of Graphene with Millimetre-Size Single-Crystal Grains Using Platinum. *Nat. Commun.* **2012**, *3*, 699.
14. Jia, C. C.; Jiang, J. L.; Gan, L.; Guo, X. F. Direct Optical Characterization of Graphene Growth and Domains on Growth Substrates. *Sci. Rep.* **2012**, *2*, 707.
15. Chen, S. S.; Brown, L.; Levendorf, M.; Cai, W. W.; Ju, S. Y.; Edgeworth, J.; Li, X. S.; Magnuson, C. W.; Velamakanni, A.; Piner, R. D.; *et al.* Oxidation Resistance of Graphene-Coated Cu and Cu/Ni Alloy. *ACS Nano* **2011**, *5*, 1321–1327.
16. Wang, H.; Wang, G. Z.; Bao, P. F.; Yang, S. L.; Zhu, W.; Xie, X.; Zhang, W. J. Controllable Synthesis of Submillimeter Single-Crystal Monolayer Graphene Domains on Copper Foils by Suppressing Nucleation. *J. Am. Chem. Soc.* **2012**, *134*, 3627–3630.
17. Shin, Y. C.; Kong, J. Hydrogen-Excluded Graphene Synthesis *via* Atmospheric Pressure Chemical Vapor Deposition. *Carbon* **2013**, *59*, 439–447.
18. Han, J. W.; Lohn, A.; Kobayashi, N. P.; Meyyappan, M. Evolutional Transformation of Copper Oxide Nanowires to Copper Nanowires by a Reduction Technique. *Mater. Express* **2011**, *1*, 176–180.
19. Kaur, M.; Muthe, K. P.; Despande, S. K.; Choudhury, S.; Singh, J. B.; Verma, N.; Gupta, S. K.; Yakhmi, J. V. Growth and Branching of CuO Nanowires by Thermal Oxidation of Copper. *J. Cryst. Growth* **2006**, *289*, 670–675.
20. Jiang, X. C.; Herricks, T.; Xia, Y. N. CuO Nanowires Can Be Synthesized by Heating Copper Substrates in Air. *Nano Lett.* **2002**, *2*, 1333–1338.
21. Zhang, Y. F.; Gao, T.; Gao, Y. B.; Xie, S. B.; Ji, Q. Q.; Yan, K.; Peng, H. L.; Liu, Z. F. Defect-like Structures of Graphene on Copper Foils for Strain Relief Investigated by High-Resolution Scanning Tunneling Microscopy. *ACS Nano* **2011**, *5*, 4014–4022.
22. Li, X. S.; Cai, W. W.; An, J. H.; Kim, S.; Nah, J.; Yang, D. X.; Piner, R.; Velamakanni, A.; Jung, I.; Tutuc, E.; *et al.* Large-Area Synthesis of High-Quality and Uniform Graphene Films on Copper Foils. *Science* **2009**, *324*, 1312–1314.
23. Gao, L.; Guest, J. R.; Guisinger, N. P. Epitaxial Graphene on Cu(111). *Nano Lett.* **2010**, *10*, 3512–3516.
24. Yan, Z.; Liu, Y.; Lin, J.; Peng, Z.; Wang, G.; Pembroke, E.; Zhou, H.; Xiang, C.; Raji, A.-R. O.; Samuel, E. L. G.; *et al.* Hexagonal Graphene Onion Rings. *J. Am. Chem. Soc.* **2013**, *135*, 10755–10762.
25. Vlassiouk, I.; Regmi, M.; Fulvio, P. F.; Dai, S.; Datskos, P.; Eres, G.; Smirnov, S. Role of Hydrogen in Chemical Vapor Deposition Growth of Large Single-Crystal Graphene. *ACS Nano* **2011**, *5*, 6069–6076.
26. Malard, L. M.; Pimenta, M. A.; Dresselhaus, G.; Dresselhaus, M. S. Raman Spectroscopy in Graphene. *Phys. Rep.* **2009**, *473*, 51–87.
27. Zhou, H. L.; Yu, W. J.; Liu, L. X.; Cheng, R.; Chen, Y.; Huang, X. Q.; Liu, Y.; Wang, Y.; Huang, Y.; Duan, X. F. Chemical Vapour Deposition Growth of Large Single Crystals of Monolayer and Bilayer Graphene. *Nat. Commun.* **2013**, *4*, 2096.